

Dark matter halo response to the disk growth

Jun-Hwan Choi, Yu Lu, H. J. Mo & Martin D. Weinberg

Department of Astronomy, University of Massachusetts, Amherst, MA 01003

jhchoi@nova.astro.umass.edu, luyu@astro.umass.edu, hjmo@nova.astro.umass.edu, weinberg@astro.umass.edu

13 October 2018

ABSTRACT

We consider the sensitivity of the circular-orbit adiabatic contraction approximation to the baryon condensation rate and the orbital structure of dark matter halos in the Λ CDM paradigm. Using one-dimensional hydrodynamic simulations including the dark matter halo mass accretion history and gas cooling, we demonstrate that the adiabatic approximation is approximately valid even though halos and disks may assemble simultaneously. We further demonstrate the validity of the simple approximation for Λ CDM halos with isotropic velocity distributions using three-dimensional N-body simulations. This result is easily understood: an isotropic velocity distribution in a cuspy halo requires more circular orbits than radial orbits. Conversely, the approximation is poor in the extreme case of a radial orbit halo. It overestimates the response a core dark matter halo, where radial orbit fraction is larger. Because no astronomically relevant models are dominated by low-angular momentum orbits in the vicinity of the disk and the growth time scale is never shorter than a dynamical time, we conclude that the adiabatic contraction approximation is useful in modeling the response of dark matter halos to the growth of a disk.

Key words: dark matter — galaxies: evolution — galaxies: halos — method: numerical

1 INTRODUCTION

In hierarchical structure formation, galaxies form in gravitationally collapsing dark matter halos. The dissipative baryonic matter cools and condenses in dark matter halo (White & Rees 1978). Blumenthal et al. (1986) described the halo response to this condensation assuming a spherical profile with circular orbits and adiabatic disk growth (Barnes & White 1984). For an adiabatic change, the angular momentum is invariant: $J^2 \propto rM(r) = \text{constant}$. Then, given the distribution of the baryonic disk $M_d(r)$ and the initial dark matter distribution $M_i(r)$, the final distribution of dark matter $M_f(r)$ must satisfy

$$\begin{aligned} M_f(r_f)r_f &= M_i(r_i)r_i \\ M_f(r_f) &= M_d(r_f) + M_i(r_i)(1 - m_d) \end{aligned} \quad (1)$$

where m_d is mass fraction of the disk. Further studies of this model include Ryden (1988, 1991), and Flores et al. (1993). Recently Jesseit, Naab & Burkert (2002) find that the adiabatic contraction approximation is in agreement with their simulations.

Despite the wide usage of the adiabatic contraction approximation, discrepancies between observations and theoretical predictions motivate a detailed check of its validity. First, Blumenthal et al. (1986) simply assumes that the disk growth time is much longer than the dark matter halo dy-

namical time. However, individual halos may grow simultaneously with their disks and have different assembly histories (Wechsler et al. 2002; Zhao et al. 2003; Li et al. 2005). Cosmological simulations of the galaxy formation have shown that gas accretion in CDM halos proceeds in two distinct modes depending on the mass of the halo (Kereš et al. 2005; Birnboim & Dekel 2003). In massive halos, gas accretion is dominated by “hot mode” in which gas is first heated up to the virial temperature of the halo and then cools to settle gradually into the halo centre. By contrast, gas accretion into small halos is dominated by “cold mode” in which cold gas sinks in a dynamical time without being shock heated. These scenarios may affect the validity of the adiabatic contraction formula. Secondly, dark matter is not arranged on circular orbits and therefore $rM(r)$ is not strictly conserved. Barnes (1987), Sellwood (1999), and Sellwood & McGaugh (2005) report that the approximation overestimates the contraction measured in simulations. Moreover, recently Gnedin et al. (2004) claimed similar findings in a cosmological simulation. These authors suggest that the discrepancy is due to the circular orbit assumption.

In this paper, we use idealised numerical experiments to investigate the effect of the two assumptions in the adiabatic contraction approximation (eq. 1) and provide physical intuition for the numerical trends. In §2, we use one-dimensional

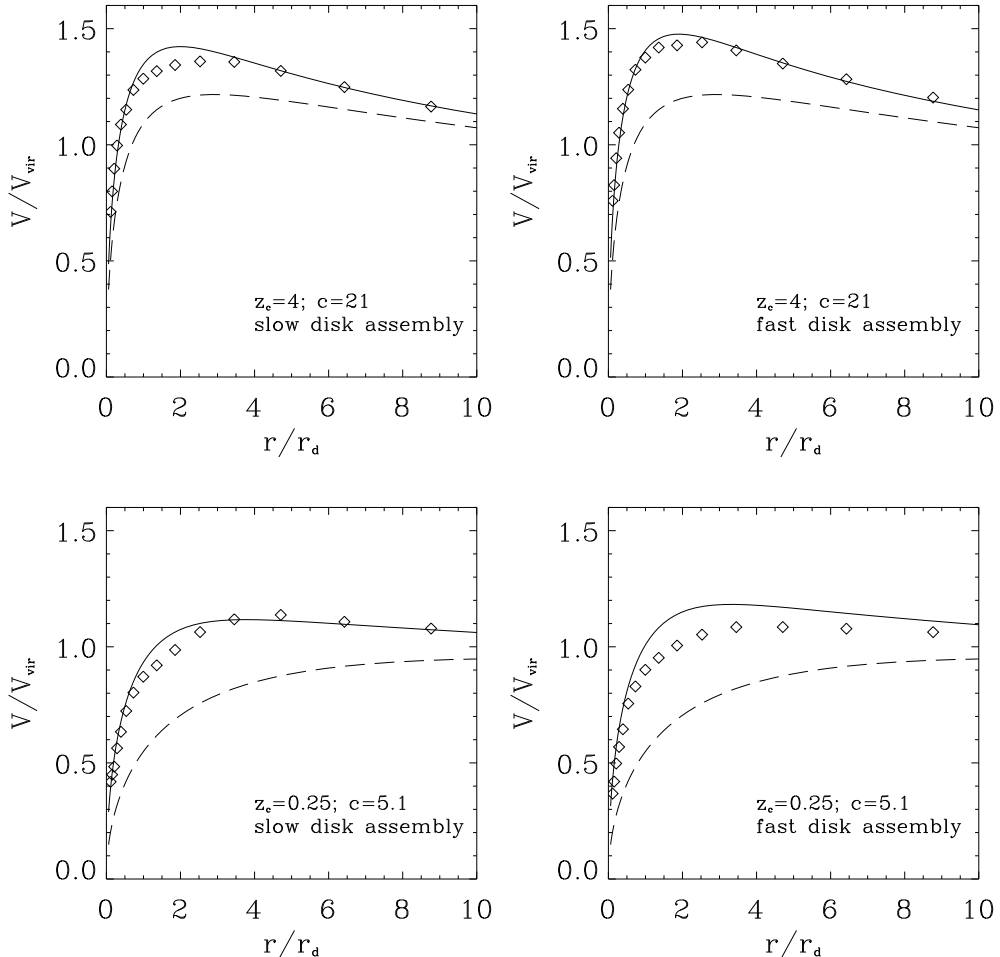


Figure 1. The rotation curves of simulated halos with different formation time and gas cooling phases compared with the rotation curves with the predictions of adiabatic contraction approximation. The upper-left panel shows the rotation curves for early-formed halo ($z_c = 4$) with normal cooling (hot mode). The upper-right panel is for early formed halo ($z_c = 4$) with artificially high cooling (cold mode). The bottom-left panel is for late formed halo ($z_c = 0.25$) with normal cooling, and the bottom-right panel is for late formed halo ($z_c = 0.25$) with high cooling. In each panel, the diamonds denotes simulation results, the solid lines show the predictions of adiabatic contraction approximation, and the dashed lines show the rotation curves of the control model, in which cooling and baryon condensation are turned off.

simulations which incorporate dark matter halo mass accretion history as well as gas cooling to test the adiabatic disk growth assumption in realistic forming halo. We find that disk growth time scale is always longer than dynamical time of the halo in many cases. We also show that the continued dark-matter mass accretion has little affect in the inner halo. In §3, we test the circular orbit assumption using high resolution N-body simulations with cosmological dark matter halo initial conditions. As expected, we find that radial orbits reduce the dark matter halo response to disk growth predicted by the simple circular-orbit approach. However, in order to maintain an isotropic velocity distribution in cuspy halos, a circular population is much larger than radial orbit population. This explains the often-observed consistency between simulations of a dark-matter cuspy halo to disk growth. We study typical CDM halos in §4 and summarise in §5.

2 ADIABATIC CONTRACTION DURING CDM HALO FORMATION

We investigate a dark matter halo response to disk growth for several different halo and disk growth time scales using one-dimensional hydrodynamic simulations (see Appendix A and Lu et al. 2006). We use 5×10^4 equal-mass shells to represent the dark matter distribution and 500 equal-mass shells to represent the gas distribution. The evolution of every gas shell is followed until it cools below 10^4 K; thereafter its mass is assigned to an exponential disk. The scale-length of the disk, r_d , is fixed to $\frac{0.05}{\sqrt{2}}r_{vir}$, where r_{vir} is the virial radius of the halo at $z = 0$ (Mo, Mao, & White 1998). The disk is assumed to be a rigid exponential disk.

We examine both an early- ($z = 4$) and late- ($z = 0.25$) time halo-formation scenarios with $M = 10^{12} M_\odot$. Because the virial mass of the halo is fixed at $10^{12} M_\odot$, gas accretion is primarily in the “hot mode” phase for this halo mass (Kereš et al. 2005). The gas is heated to the virial tempera-

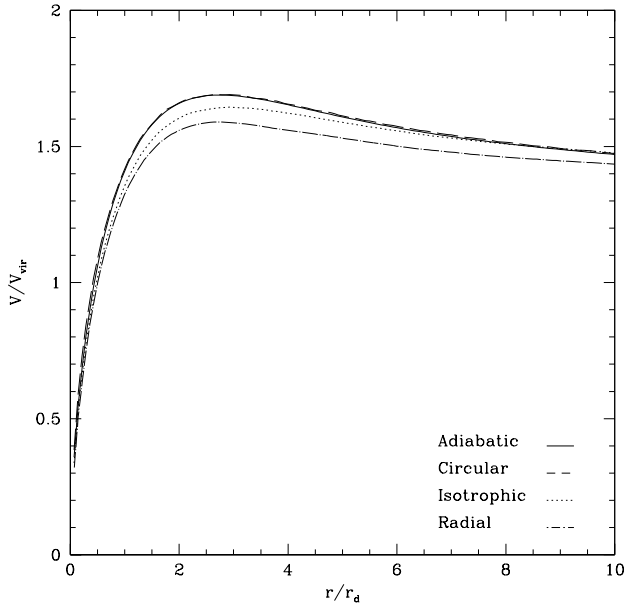


Figure 2. The final rotation curve for a circular orbit (long-dashed), an isotropic (dotted), and a radial-orbit dominant (dot-dashed) distribution. The dark matter halo is $c=12$ NFW halo and disk is fiducial disk. The solid line is for the adiabatic contraction approximation prediction. The rotation curve for the adiabatic contraction approximation prediction and the circular orbit halo case are almost identical.

ture and then slowly cools to form a disk. In order to examine the adiabatic contraction for the “cold mode” gas accretion, we artificially increase cooling rate by a factor of 100. Then, the accreted gas cools rapidly and joins the disk without shock heating. In this case, the disk and its host halo have similar growth times.

For the four simulations, two redshifts and two accretion models, we measure the rotation curves at the present time, which are shown in Figure 1. Since disk growth time is longer than dynamical time of the dark matter halo in all four, the adiabatic contraction approximation adequately predict the response of dark matter halos. Although the host halo continues to accrete dark matter, this accretion primarily affects the outer halo. In summary, the adiabatic contraction formula gives an acceptable approximation for these standard scenarios.

3 ADIABATIC CONTRACTION FOR A NON-CIRCULAR ORBIT DISTRIBUTION

We explore disk growth in a dark matter halo represented by a Navarro, Frenk & White (1997, hereafter NFW) profile, $\rho \propto 1/[r(r+r_s)^2]$ with virial radius r_{vir} . We assume a concentration $c = r_{vir}/r_s = 12$ consistent with the rotation curve for a large spiral galaxy and examine three cases of different anisotropy to study the effects of radial orbits on the circular-orbit adiabatic prediction: a circular-orbit halo, an isotropic halo, and a radial orbit biased halo. The NFW halo with pure circular orbits is constructed by assigning each of the particles at radius r a tangential velocity, $v_c = \sqrt{GM(< r)/r}$

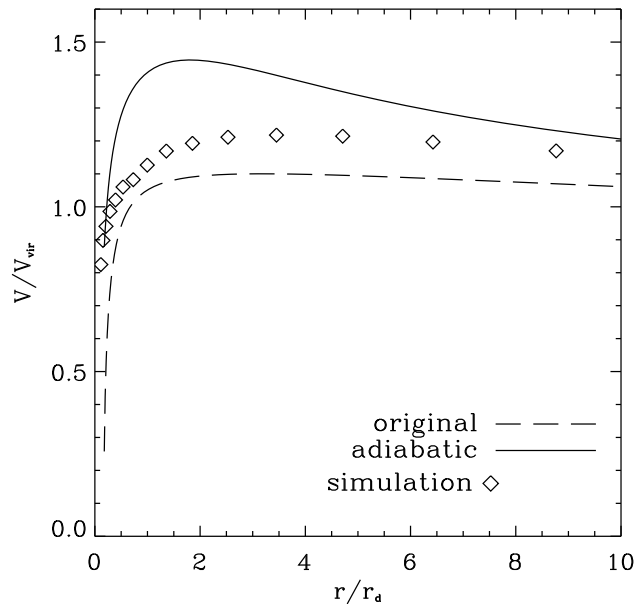


Figure 3. The rotation curve of the pure radial orbit halo. The diamonds denote the simulation result, the solid line denotes the prediction of adiabatic contraction, and the long dashed line denotes the rotation curve of the reference halo.

in a random tangential direction. The isotropic and radially biased distribution functions are computed using the Osipkov-Merritt model (Binney & Tremaine 1987; Osipkov 1979; Merritt 1985) which controls the orbital structure by an anisotropy radius r_a . For an isotropic halo, $r_a = \infty$. For the radially biased case, we choose the minimum value for r_a that results in positive density. The anisotropy profile in this model closely corresponds to the profile from a virialized collapse (Eke, Navarro & Frenk 1998; Colín, Klypin & Kravtsov 2000). The $N = 10^6$ -particle phase spaces are realized by a Monte Carlo procedure. Our rigid exponential disk has mass $m_d = 0.04M_{vir}$ and the disk scale length is $r_d = 0.014r_{vir}$ motivated by galaxy formation in Λ CDM cosmogony (Mo, Mao, & White 1998; Klypin, Zhao & Somerville 2002). To mimic disk growth, we increase the disk mass from zero, keeping the disk scale length unchanged. To ensure the validity of the adiabatic approximation, the time scale of disk mass growth is 10 times longer than the dynamical time of the dark matter halo at the disk scale length. The gravitational force on each dark matter particle is calculated using the self-consistent field code (SCF) (Clutton-Brock 1972, 1973; Hernquist & Ostriker 1992; Weinberg 1999), which solves Poisson’s equation using a set of density-potential bi-orthogonal function expansions.

Figure 2 shows the total rotation curves after disk contraction for the circular orbit case (long dashed curve), the isotropic case (dotted curve) and the radial orbit biased case (dot-dashed curve). For comparison, we also show the prediction of the adiabatic contraction approximation (solid curve). The adiabatic contraction approximation is nearly exact for circular orbits, but overestimates the contraction when the eccentric orbit contribution increases. The radial orbit biased halo model is not significantly biased toward radial orbit around disk ($r_a = 0.1r_{vir} \simeq 7r_d$). Consequently

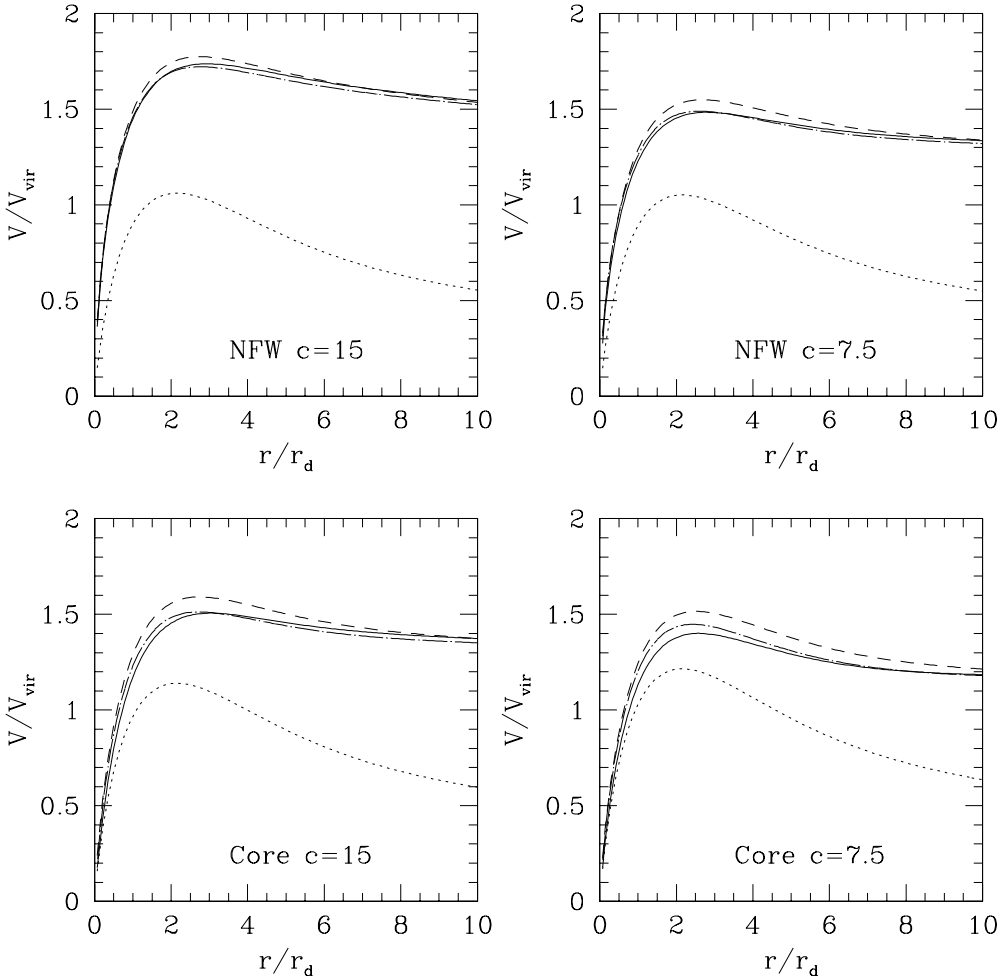


Figure 4. Rotation curves from simulations cooperated with the adiabatic contraction approximation for isotropic NFW and core halos. The dotted line is the rotation curve from disk only, the solid line is the total (disk + dark matter halo) rotation curve from the simulation results, and the long dashed line is the total rotation curve from the adiabatic contraction approximation. We also plot the total rotation curve predicted by the modified adiabatic contraction approximation of Gnedin et al. (2004) with $A = 0.85$ and $w = 0.8$ (dot-dashed line). The disk has the fiducial parameters: $r_d = 0.014r_{vir}$ and $m_d = 0.04m_{vir}$. The overestimation by the adiabatic contraction approximation increases as halo concentration decreases. The modified adiabatic contraction approximation provides a much better fit to the simulation results.

the effect of radial orbit is not dramatic in Figure 2. However it is clear that the radial orbit reduces the dark matter halo response.

Since it is difficult to simulate pure radial orbit halos in three-dimensional N-body simulation, we use implement one-dimensional simulation with a pure radial orbit halo. The orbits are purely radial and the density profile of the simulated halo is proportional to r^{-2} in central region. Figure 3 shows the rotation curve of the simulated halo compared with the prediction of adiabatic contraction formula. The circular-orbit prediction overestimates the contraction by factor of two.

4 ADIABATIC CONTRACTION FOR TYPICAL CDM HALOS

We consider a range of halo parameters and disk masses to explore the general applicability of the circular-

orbit adiabatic approximation. Recent cosmological simulations show that velocities in the inner region of dark matter halos is isotropic (Eke, Navarro & Frenk 1998; Colín, Klypin & Kravtsov 2000; Fukushige & Makino 2001; Diemand, Moore & Stadel 2004). Therefore we explore isotropic halos. Although an NFW halo model is currently accepted in CDM cosmology, some recent theoretical models (Mo & Mao 2002, 2004; Oh & Benson 2003; Weinberg & Katz 2002) and observations (De Blok et al. 2001) suggest that dark halos may have cores. Simulations for the core halo are also carried for the three cases, with $c \equiv r_{vir}/r_{core} = 15, 12$, and 7.5 , respectively. In addition to the fiducial disk, $m_d = 0.04M_{vir}$ and $r_d = 0.014R_{vir}$, we consider a low-mass ($m_d = 0.02M_{vir}$) and a high-mass ($m_d = 0.1M_{vir}$) disk.

Figure 4 compares the post-formation rotation curves for NFW halos and core halos with $c = 15$ and $c = 7.5$ with the adiabatic contraction predictions. The formula overestimates the rotation velocity for these astronomically mo-

tivated halo models although the discrepancy is modest. Figure 5 quantifies the relative differences, $\eta \equiv |V_{ad} - V_{sim}|/V_{sim}$, as a function of halo concentration c , where V_{sim} and V_{ad} are the circular velocities at $r = 2.2R_d$ obtained from simulation and from the adiabatic contraction (eq. 1), respectively. The discrepancy is 4% for NFW model with $c = 15$ and increases to 8% for $c = 7.5$. The discrepancy increases with disk mass but the dependence is weak. The $c = 7.5$ case is a low value for galaxy halos in the current CDM model, therefore, these results show that the adiabatic contraction approximation remains good for isotropic NFW halos. For core halos, the discrepancy is 14% for $c = 15$ and increases to 23% for $c = 7.5$ with weak dependence on m_d .

Gnedin et al. (2004) improved the agreement between the adiabatic contraction approximation and the simulation result using a modified version of the original adiabatic contraction approximation including the effect of non-circular orbits. In this model, the adiabatic invariant $M(r)r$ is replaced by $M(\bar{r})r$, where $\bar{r} = Ar^w$. The authors suggested $A \approx 0.85 \pm 0.05$ and $w \approx 0.8 \pm 0.02$ based on cosmological dark matter halo simulations. As comparison, we show in Figure 4 the rotation curves obtained from this modified adiabatic contraction approximation, together with those obtained from the simulation and from the original adiabatic contraction approximation. As one can see, the modified adiabatic contraction approximation agrees with the simulation results for NFW halos. For halos with a constant density core, there is clear discrepancy between the model and simulation, although the modified model is better than the original adiabatic contraction model. Although the Gnedin et al. (2004) model takes the effect of non-circular orbits into account, their fitting formula, $\bar{r} = Ar^w$, is not based on the orbital structure. It simply reduces the halo contraction using fitting formula with empirically suggested fitting parameters. Therefore the Gnedin et al. (2004) model estimation for core halo cases with suggested fitting parameters does not work as well as one for NFW halo cases. For core halo, different fitting parameters and further modification in fitting formula are required.

Figure 5 shows that the adiabatic contraction approximation is better for high-concentration halos. This trend is explained by the distribution of orbits. We describe the shape of an orbit by the ratio of the angular momentum to the angular momentum of a circular orbit at a fixed energy $\kappa = J/J_{max}(E)$. The orbit with $\kappa = 0$ ($\kappa = 1$) is radial (circular). Figure 6 describes the ensemble average of this ratio for isotropic halo in radial bins $\langle \kappa \rangle(r)$. At a fixed energy, the mean value of κ is $2/3$ for comparison.

Figure 6 shows that an isotropic NFW halo has more low-eccentricity orbits at fixed radius than an isotropic core halo. This can be understood as follows. The density at a given radius in a halo is contributed by particles on different orbits. In the inner region of a halo, orbits with lower energies are more circular, while those with higher energies are more radial. Assuming isotropic velocity dispersion, one can show that the energy distribution is flatter in a core halo than in a cuspy halo. Consequently, for isotropic velocity distribution a core halo requires more high-eccentricity orbits than an NFW halo.

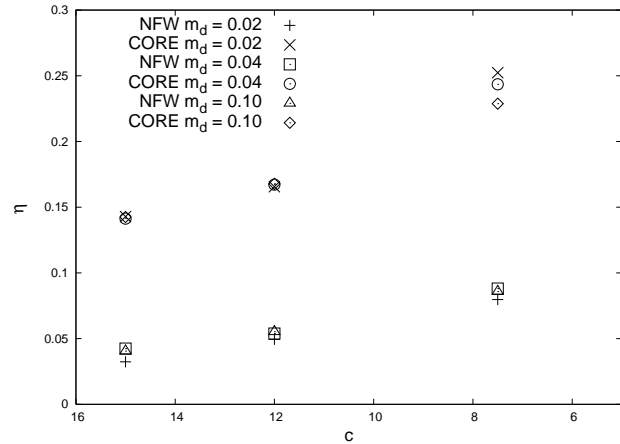


Figure 5. Relative difference ($\eta = \frac{|V_{ad}| - V_{sim}|}{V_{sim}}$) between the rotation speed from the simulation and from the adiabatic contraction approximation at $2.2R_d$ for $c=15, 12$, and 7.5 NFW and core halos. Three disks, $m_d = 0.1, 0.04$, and $0.01 M_{vir}$, are considered for each halo. The relative difference depends strongly on the halo structure and the disk mass dependence is negligible.

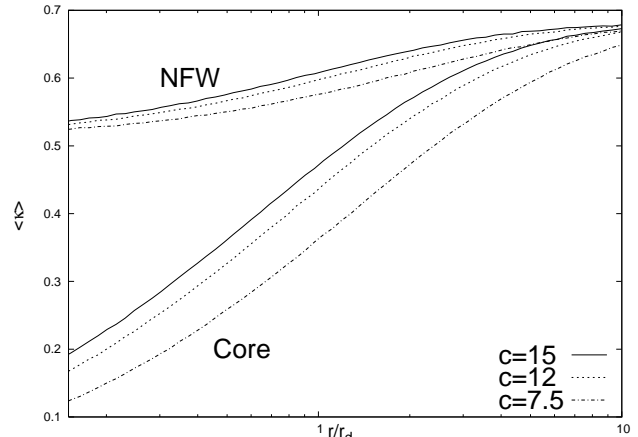


Figure 6. The mean relative angular momentum per orbit, $\kappa = J/J_{max}(E)$, is averaged in radial bins for both the NFW and core halo models and three concentrations. The top three lines represent NFW halo models and bottom three lines represent core halo models. The solid lines show $c=15$ NFW and core halo models, the dotted lines show $c=12$ halo models, and dot-dashed lines show $c=7.5$ halo models. The fraction of eccentric orbits increases dramatically in core halos.

5 SUMMARY

We study the accuracy of the circular-orbit adiabatic approximation (Blumenthal et al. 1986) in predicting halo contraction due to disk formation and provide a physical explanation for the deserved trends. We consider: (1) variation in the accretion time scale; (2) variation in the accreted disk mass; (3) variation in the central concentration of both cuspy and core halo models; and (4) variation in the velocity isotropy. The circular orbit adiabatic contraction approximation is acceptable over a wide range of astronomically interesting parameters. The relative change in the rotation curve value between the simulation and circular orbit approximation at 2.2 disk scale lengths, η , is less than 23%

for our entire range of realistic parameters. We find that the disk growth is still slower than dark matter halo dynamical time in the vicinity of the disk and therefore the adiabatic approximation is maintained. The value of η depends only weakly on the fraction of accreted baryon mass, and therefore, the dependence on halo concentration cannot be explained by disk dominance in less concentrated halos. However, η is strongly correlated with the fraction of eccentric orbits in the distribution. The steeper the cusp, the larger fraction of more circular orbits are required at *fixed* radius, and this supports the circular orbit approximation. Although the adiabatic concentration approximation overestimates the response of dark matter halos, as long as the dark matter halo has central cusp and isotropic velocity distribution the overestimation is negligible.

Our results have important implications for the formation of disk galaxies in the CDM scenario. In comparing theory with the observed Tully-Fisher relation, one usually uses the peak rotation velocity of galaxy disks to represent the observed rotation velocities (Mo, Mao, & White 1998). However, as shown in Mo & Mao (2000), if dark matter halos respond to the disk growth according to the adiabatic contraction model, current CDM model predicts a Tully-Fisher relation that has a much too low zero-point (i.e. galaxies are too faint for a given peak rotation velocity). In order to match the observed Tully-Fisher zero-point, one has to assume that disk growth does not cause any contraction in dark matter halos at all (Croton et al. 2006, e.g.). This assumption is not supported by our results, which show that adiabatic contraction approximation works reasonably well for CDM halos over a wide range of situations. However, it should be pointed out that there are other astrophysical processes, such as mergers (Dekel, Devor, & Hetzroni 2003; Boylan-Kolchin & Ma 2004), dynamical heating by substructures (El-Zant et al. 2004), halo pre-processing (Mo & Mao 2004), and resonance dynamics (Weinberg & Katz 2002), that may modify halo structures but are not included in the models considered here. Unfortunately, the importance of these processes are not well understood at the present.

ACKNOWLEDGEMENTS

We would like to thank our referee, Joel Primack, for many comments and suggestions that improved this paper. We would like to thank Neal Katz for useful discussions. JHC and YL thank Dusan Kereš and Yicheng Guo for reading our manuscript. MDW acknowledges the support of NASA ATP NAG5-12038.

REFERENCES

Barnes, J. & White, S. D. M. 1984, MNRAS, 211, 753
 Barnes, J. 1987, in *Nearly Normal Galaxies: From the Plank Time to the Present*, ed. S. A. M. Faber (New York: Springer-Verlag) p.154
 Binney, J. & Tremaine, S. 1987, *Galactic Dynamics*. Princeton Univ. Press Princeton
 Birnboim, Y. & Dekel, A. 2003, MNRAS, 345, 349
 Blumenthal, G. R., Faber, S. M., Flores, R. & Primack, J. R. 1986, ApJ, 301, 27
 Boylan-Kolchin, M. & Ma, C. 2004, MNRAS, 349, 1117
 Colín, P., Klypin, A. A. & Kravtsov, A. V. 2000, ApJ, 2000, 539, 561
 Croton, D. J., Springel, V., White, S. D. M., De Lucia, G., Frenk, C. S., Gao, L., Jenkins, A., Kauffmann, G., Navarro, J. F. & Yoshida, N., 2006, MNRAS, 365, 11
 Clutton-Brock, M. 1972, Ap&SS, 16, 101
 Clutton-Brock, M. 1973, Ap&SS, 23, 55
 De Blok, W. J. G., McGaugh, Stacy S. & Rubin, Vera C. 2001, AJ, 122, 2396
 Dekel, A., Devor, J. & Hetzroni, G. 2003, MNRAS, 341, 326
 Diemand, J., Moore, B., & Stadel, J. 2004, MNRAS, 352, 535
 Eke, V. R., Navarro, J. F., & Frenk, C. S. 1998, ApJ, 503, 569
 El-Zant, A., Hoffman, Y., Primack, J., Combes, F., & Shlosman, I. 2004, ApJ, 607, L75
 Flores, R., Primack, J. R., Blumenthal, G. R., & Faber, S. M. 1993, ApJ 412, 443
 Fukushige, T. & Makino, J. 2001, ApJ, 557, 533
 Gnedin, O. Y., Kravtsov, A. V., Klypin, A. A. & Nagai, D. 2004, ApJ, 616, 16
 Herquist, L. & Ostriker, J. P. 1992, ApJ, 386, 375
 Jesseit, R., Naab, T. & Burkert, A. 2002, ApJ, 571, L89
 Katz, N., Weinberg, D. H. & Hernquist, L. 1996, ApJSS, 105, 19
 Kereš, D., Katz, N., Weinberg, D. H. & Davé, R. 2005, MNRAS, 363, 2
 Klypin, A., Zhao, H. & Somerville, R. S. 2002, ApJ, 573, 597
 Li, Y., Mo, H.J., van den Bosch, F. C., 2005, preprint (astro-ph/0510372)
 Lu, Y., Mo, H.J., Katz, N. & Weinberg, M.D., 2006, MNRAS, 368, 1931
 Merritt, D. 1985, AJ, 90, 1027
 Mo, H. J. & Mao, S. 2000, MNRAS, 318, 163
 Mo, H. J. & Mao, S. 2002, MNRAS, 333, 768
 Mo, H. J. & Mao, S. 2004, MNRAS, 353, 829
 Mo, H.J., Mao, S. & White, S. D. M., 1998, MNRAS, 295, 319
 Navarro, J. F., Frenk, C. S. & White, S. D. M. 1997, ApJ, 490, 493
 Oh, S. P. & Benson, A. J. 2003, MNRAS, 342, 664
 Osipkov, L. P. 1979, Pis'ma Astr. Zh., 5, 77
 Ryden, B. S. 1988, ApJ, 329, 589
 Ryden, B. S. 1991, ApJ, 370, 15
 Sellwood, J. A. 1999, in Merritt D., Sellwood J. A., Valluri M., eds, ASP Conf. Ser. Vol. 182, *Galaxy Dynamics : A Rutgers Symposium*. Astron. Soc/ Pac., San Francisco, p. 351
 Thoul, A. & Weinberg, D. H. 1995, ApJ, 442, 480A
 Sellwood, J. A., & MaGaugh, S. S. 2005, ApJ, 634, 70
 Weinberg, M. D. 1999, AJ, 117, 629
 Weinberg, M. D. & Katz, N. 2002, ApJ, 580, 627
 Wechsler, R. H., Bullock, J. S., Primack, J. R., Kravtsov, A. V., Dekel, A., 2002, ApJ, 568, 52
 White, S. D. M. & Rees, M., 1978, MNRAS, 183, 341
 Zhao D., Mo H. J., Jing Y. P., Börner G., 2003, MNRAS, 339, 12

APPENDIX A: ONE-DIMENSIONAL HYDRODYNAMIC SIMULATIONS

We use the Lagrangian based one-dimensional hydrodynamic code described in Lu et al. (2006) to simulate formation of a halo from an initial perturbation at a high redshift z_i . We assumes the halo mass accretion histories proposed by Wechsler et al. (2002)

$$M(a) = M_0 \exp \left[-2a_c \left(\frac{a_0}{a} - 1 \right) \right], \quad (\text{A1})$$

where a is the expansion scale factor, a_c is the scale factor corresponding to the formation time of the halo, and M_0 is mass of the halo at the observation time a_0 . In this function, a_c is the only free parameter to characterize the shape of a mass accretion history. Reader may refer to Lu et al. (2006) for detailed description on making the initial conditions given the mass accretion history. We choose $z_i = 200$, and the initial temperature of gas shells is set to be the CMB temperature at this epoch.

The simulation has both dark matter shells and gas shells. The gas initially follows the distribution of the dark matter but evolves differently from the dark matter due to hydrodynamics. We use the Lagrangian finite-difference scheme to follow the evolution of the shells. The numerical treatment is same as what is described in Thoul & Weinberg (1995). To avoid numerical instability due to dark matter shell-crossing, the mass of each dark matter shell is chosen to be much smaller than that of a gas shell. The baryon fraction is fixed at $f_b = 0.17$. The chemical abundance is assumed to be primordial. The radiative cooling function proposed by Katz et al. (1996) is implemented in the simulations.

When a gas shell cools to a temperature, below 10^4 K, the gas in the shell is considered to be cold. Since we do not include any cooling processes below this temperature, the cold gas is assumed to retain a temperature of 10^4 K until it flows into the center of the halo. At this point, the gas joins a central exponential disk with a scalelength $r_d = \frac{0.05}{\sqrt{2}} r_{\text{vir}}$, where r_{vir} is the virial radius of the halo at $z = 0$. The cold gas disk is assumed to be a rigid object, and its gravity is included in the subsequent evolution of other mass shells. At any given time, the gravitational acceleration of a shell at radius r_i is given by

$$g_i = H_0^2 \Omega_\Lambda r_i - \frac{GM(< r_i)r_i}{(r_i^2 + r_\alpha^2)^{3/2}}, \quad (\text{A2})$$

where H_0 is the Hubble's constant at the present time, Ω_Λ is the density parameter of the cosmological constant, $M(< r_i)$ is the total mass (dark matter, gas and exponential disk) enclosed by r_i , and α is a softening length taken to be 0.0005 of the virial radius of the halo at the present time. This scale is much smaller than any scale of interest. In the simulations, the density parameter of the non-relativistic matter and of the cosmological constant are $\Omega_M = 0.3$ and $\Omega_\Lambda = 0.7$. and the Hubble's constant is $H_0 = 100 \text{km s}^{-1} \text{Mpc}^{-1}$.